Available online at www.sciencedirect.com
SCIENCE DIRECT®
Microelectronic Engineering 77 (2005) 103–109
MICROELECTRONIC ENGINEERING
www.elsevier.com/locate/mee

Illinois debris-mitigation EUV applications laboratory

B.E. Jurczyk, E. Vargas-Lopez *, M.N. Neumann, D.N. Ruzic

Plasma-Material Interaction Group, Department of Nuclear, Plasma and Radiological Engineering, University of Illinois, 103 S Goodwin Avenue, Urbana-Champaign, Urbana 61801, USA

Received 9 April 2004; received in revised form 28 July 2004; accepted 1 September 2004
Available online 12 October 2004

Abstract

Gaseous discharge light sources are leading candidates for generating 13.5 nm wavelengths needed for next-generation optical lithography. Electrode debris reaching the first collector optic is a serious concern for device lifetime and cost of ownership. This paper describes the experimental setup and initial data obtained for testing secondary-plasma-based debris mitigation for EUV gas discharge light sources. Operation of a dense plasma focus, secondary RF debris mitigation system, and several in situ diagnostics were successfully tested, achieving first measurements for debris attenuation. It was also found that fast ion and fast neutral particle erosion processes at the optical mirror location dominate over deposition of sputtered metal if a collimator or "foil trap" is positioned between the hot pinch plasma and the first collector optic.

Keywords: EUV; Lithography; RF plasma; Dense plasma focus; DPF; EUV; Debris mitigation; EUV source

1. Introduction

Discharge plasma light sources, such as the dense plasma focus, are leading candidates for EUV. These units rely on intense currents and plasma sheath compression in close proximity to electrode surfaces. Plasma-material interactions at these surfaces generate debris in the form of sputtered electrode material, metal flaking, localized melting, etc. Next-generation EUV photolithography machines (>25 kW-class) require the integration of multiple order-of-magnitude improvements in debris removal to achieve needed component lifetime and operational stability [1]. Current debris removal systems for low-power sources utilize buffer gases and debris shields to limit material reaching optical surfaces. Under high-volume manufacturing conditions, debris loading would become too great forcing frequent change-outs and machine down

* Corresponding author. Tel.: +1 6306776520; fax: +1 2173332906.
E-mail address: vargaslo@uiuc.edu (E. Vargas-Lopez).

0167-9317/$ - see front matter © 2004 Elsevier B.V. All rights reserved.
doi:10.1016/j.mee.2004.09.006

time in the fab. Therefore, innovative debris removal schemes are needed to extend or augment the capabilities current systems to approach a >10,000 h operational lifetime.

The Illinois Debris-mitigation EUV Applications Laboratory (IDEAL) was constructed to test and validate advanced debris mitigation techniques. The IDEAL facility utilizes a dense plasma focus discharge source operating at nominal conditions of 15 J/pulse, 30 Hz rep rate, and 3 kV. Industrial gas discharge light sources under development by Cymer, Xtreme, and Philips generate 13.5 nm light through z-pinch heating of xenon gas [2–4]. Argon gas has been tested to generate plasma environmental conditions similarly experienced by industry. Additionally, argon is routinely used in industry as a debris buffer shield to slow down and scatter advancing high-energy ions from reaching the optical mirrors.

An innovative secondary-plasma-based debris mitigation technique is presented; based on a concept pioneered from iPVD reactors at the University of Illinois [5]. Electrode and chamber component sputtered debris is re-ionized in the secondary plasma region and removed with the application of electric fields prior to the collection optics. An internal helical resonator inductive coil generates the secondary plasma with minimal coil self-biasing for decreased erosion [6]. The plasma field generated by the high power RF serves to affix charge onto debris materials and ionize neutral species for direction into a foil collector. This can be accomplished with a small voltage bias or natural sheath potential forming around the debris collector tool; this process works in conjunction with the foil trap at removing large particulates and clusters. The secondary plasma also can serve as a pre-ionization source for the DPF device, enhancing pinch uniformity. Also, the plasma source can be used for refreshing the foil trap surfaces during maintenance cycles with a sputtering bias potential and flowing gas, since the debris foils will accumulate material over time and lose optical transparency.

This paper serves as an introduction to IDEAL, initial experimental results from the DPF operation and measured debris time of flight.

2. Experimental setup

IDEAL is built around a multiport 40-cm diameter, 40-cm length stainless steel vacuum vessel. A Varian 300 L/s turbomolecular pump and Ebara high-throughput roughing pump provide gas regulation combined with an integrated MKS Baratron variable gate-valve and HTS mass flow controller. Due to large o-ring seals, the base pressure on the system is 1×10^{-6} Torr.

As shown in Fig. 1, the dense plasma focus configuration is obtained by two co-axial electrodes mounted vertically center in the chamber. The

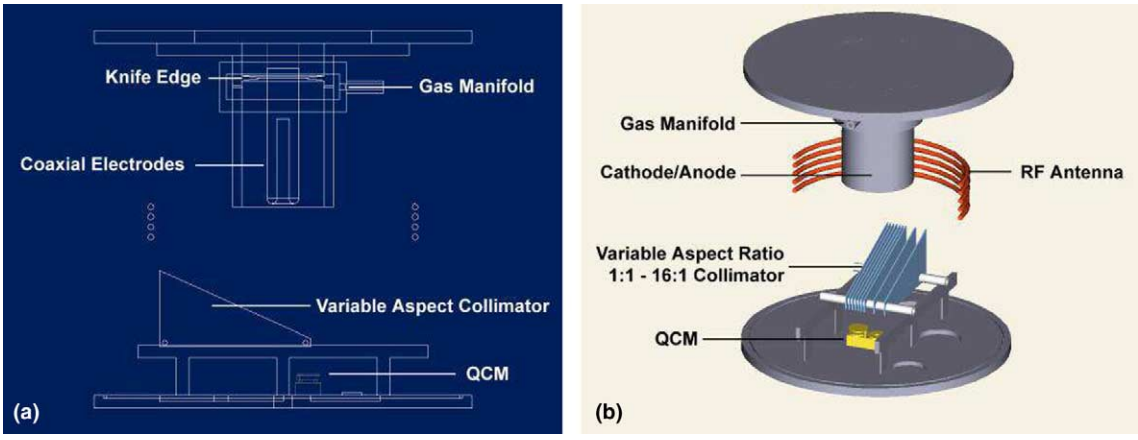

Fig. 1. (a, b): Scale cut-through drawing of coaxial electrode dense plasma focus and 3D view of variable aspect collimator.

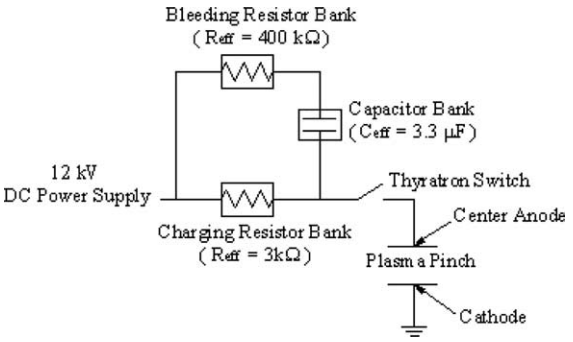

Fig. 2. Electrical circuit diagram for RF and DPF system.

outer electrode (cathode) is aluminum with 8.25-cm inner diameter with 12-cm length. The inner electrode (anode) is 3.15-cm diameter copper with a high-voltage feedthrough connection connecting to the external circuit.

A Triton F-211 hydrogen thyratron provides the high-voltage, high-current switching capability. A custom 12 kW charging supply feeds a set of ten parallel Cornell–Dublier 0.333 F capacitors with an intrinsic inductance of 50 nH each, as shown in Fig. 2. A Pearson 301X integrating coil measures the actual current through the DPF. An Oregon Analog PHV4002 high-bandwidth probe measures the anode voltage after the thyratron switch.

To facilitate discharge initiation, gas is injected into the region between the electrodes through a series of eight pinholes located at the electrode base, knife-edge and insulator junction. A gas manifold distributes the pressure equally around each inlet for uniform high-density plasma formation. High purity argon is used as the working gas to generate representative plasma conditions; xenon gas can be fed as a gas mixture or injected through the anode tip through a separate gas feedthrough for EUV emission.

The primary diagnostic is an Inficon dual quartz crystal microbalance (QCM) mounted on the bottom chamber flange. The dual microbalance has one crystal always shuttered providing an in-situ reference that minimizes thermal, vibration and electrical noise effects, since the difference between the two crystals is used to determine to determine the erosion or deposition rate [7]. The QCM is located approximately 20 cm from the

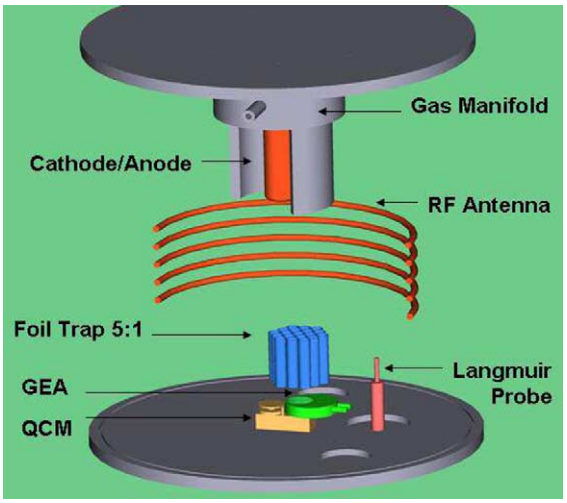

Fig. 3. Experimental diagram of interior of IDEAL chamber showing 5:1 hexagonal array of tubular foil trap.

plasma pinch region and can be mounted either directly the z-axis (below the pinch) or off-axis to measure deposition. A collimator (foil trap) is located above the QCM on a linear-motion feedthrough. Two foil traps were tested on IDEAL. One consists of a series of interleaving biasable foils with aspect ratios of 1:1–16:1, as shown in Fig. 1, and the other is a series of stainless steel tubes welded into a hexagonal pattern with a 5:1 length to diameter ratio, as shown in Fig. 3.

The secondary plasma generation region is defined by a five-turn immersed RF coil placed between the electrode exit plane and the top of the foil trap. The coil is constructed from five-turns of 0.6-cm diameter rigid copper tubing with a length of ~3.7 m. The coil operates in 1/4 wavelength mode for 13.56 MHz and 1/2 wavelength mode for 27 MHz, as illustrated in Fig. 4. Two Sprague 1500 μF blocking capacitors isolate the internal coil from the RF generator and is tuned through a pi matching network. An ENI A-500 power amplifier drives the selectable RF frequency and amplitude into IDEAL chamber from a BK Precision oscillator.

A RF-compensated Langmuir probes measure the local plasma density and temperature in the central bulk plasma region [8]. An isolated bipolar Kepco programmable power supply provides a linear ramp bias to the probe tip while floating at the

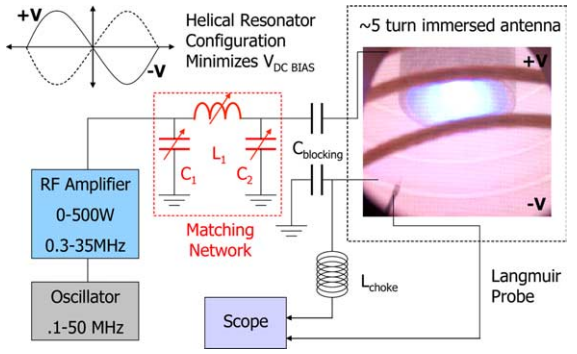

Fig. 4. Secondary plasma circuit illustration for generating and sustaining the plasma and for measuring the parameters: n_e, T_e, V_{bias} and V_{plasma}.

sheath voltage. An Agilent Infinium 54845B 1 GHz digital storage oscilloscope records the probe response. Figs. 5(a)–(b) show the results from RF plasma operation at 10W input power at 27 MHz. The floating $V_{DC\,BIAS}$ of the coil is measured through the oscilloscope or a handheld Fluke multimeter through an RF choke.

3. Results

The Langmuir probe results of the secondary plasma indicated an electron density of $n_e = 2.1 \pm 0.2 \times 10^{11}$ cm^{-3} and $T_e = 4.1 \pm 0.2$ eV. The floating potential was $14 + 1$ V, and the plasma potential was $26 + 1$ V. These values are typical for helical resonator-genreated plasmas.

The DPF is operated between 1 and 50 Hz at a voltage of 3 kV applied across the switch and plasma load during firing of the device. Fig. 6 shows a typical I–V waveform trace. Voltage is applied across the coaxial electrodes leading to surface breakdown and plasma formation across the insulator in phase II. Liftoff and rundown of the plasma sheath occurs during phase III characterized by a large increase in current. The plasma reaches the end of the anode tip and pinches at phase IV, followed by expansion of the plasma into the main chamber.

From Fig. 6, it is apparent from the I–V trace that the pinch phase occurs early in the current pulse, not achieving maximum compression which is dependent on I^2. This is due to the inherent large system inductance limiting the current rise time in conjunction with a modest electrode length. In future development, the inductance will be decreased and optimized with electrode length such that the plasma sheath arrives at the electrode tip at or slightly after peak current. Compared to commercial EUV system developers, the IDEAL pulse length is a factor of five times longer [2]. Shorter pulse lengths are achieved in commercial sources through magnetic pulse compression and IGBT switching to arrive at large amplitude short pulse widths. However, for generating representative debris the IDEAL system was found to be comparable to reports from industry showing multi-charge-stage fast ions and sputtered electrode material.

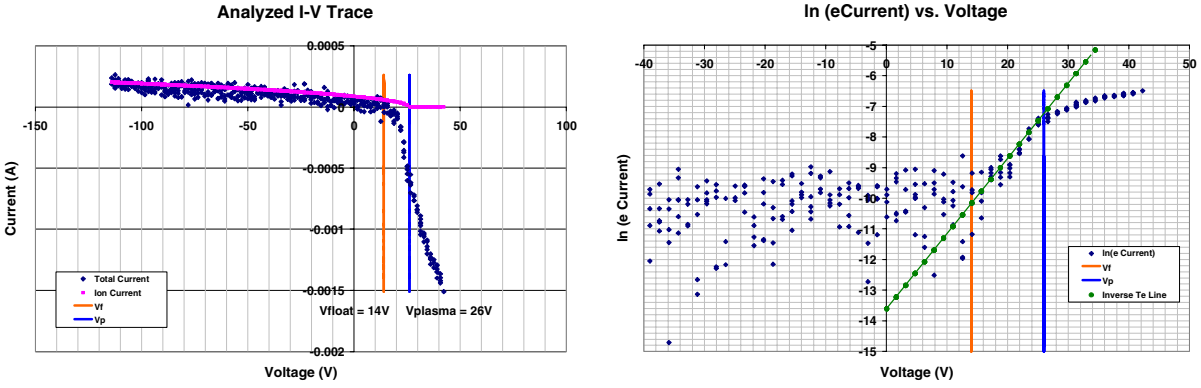

Fig. 5. (a)–(b): Analyzed Langmuir probe data showing $n_e = 2.1 \times 10^{11}$ cm^{-3} and $T_e = 4.1$ eV.

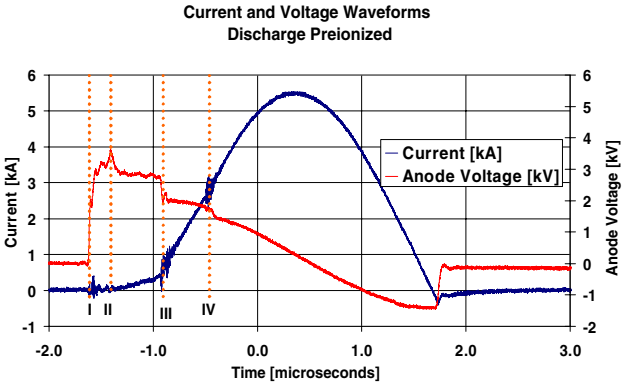

Fig. 6. DPF waveform current and voltage illustrating stages of discharge evolution from (I) switch closure, (II) surface breakdown, (III) plasma liftoff and rundown, (IV) pinch phase, and expansion at later times.

Fig. 7 shows a representative signal from an ion detector placed just above the QCM location measuring time-of-flight. Operation at 3 kV shows a peak in the fast ion signal corresponding to arrival the of 5.5 keV ions. At the time of the pinch, the voltage on the center electrode for this discharge was 1870 V. At 2.5 kV operation, the ion signal peak is shifted to lower energies indicating the arrival of 4.1 keV ions. During this experiment, the voltage was at 1400 V at the time of the pinch. The ratios of these voltages leads us to conclude that the dominant ion species expelled from the pinch was Ar^{3+}.

Components of debris including fast ions (erosion) and sputtered electrode debris material (deposition) were measured at the QCM. Fig. 8 illustrates the debris model developed to cross-correlate data and evaluate the effectiveness of the secondary plasma debris mitigation system. There are two fast ion components generated at different

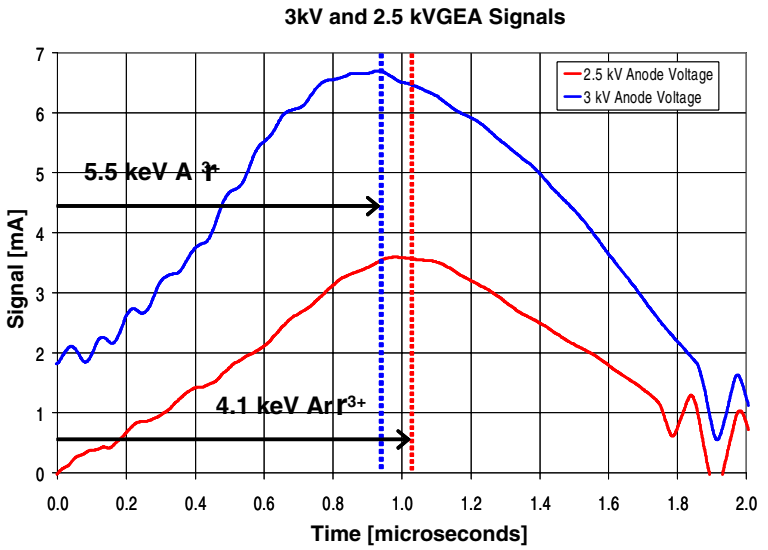

Fig. 7. Operation at 3 and 2.5 kV shows delay in peak of detector signal and magnitude. Time of flight correlation with applied pinch voltage yield estimates of 3+ charge state argon ions arriving at the detector position.

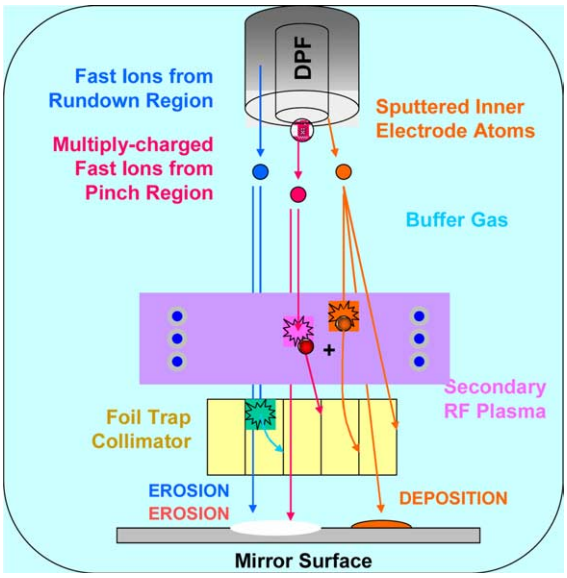

Fig. 8. Illustration of debris field and formation mechanisms, in conjunction with mitigation techniques installed in IDEAL.

places. There is also a diffusive like deposition flux of sputtered material. By varying the position of the QCM and inserting the foil trap the components can be isolated. The results of those experiments are published in our accompanying paper [9].

The application of secondary plasma between the DPF pinch location and the QCM produced measurable effects on debris deposition at the QCM monitor. Fig. 9 provides data for the variable-aspect collimator in the 3:1 position for application of low-power 10 W RF secondary plasma. The debris deposition rate decreases by 30%. Placing alternating biasing (+100 V) on the collimator plates produced no measurable effect on deposition or erosion, suggesting that the fast ion trajectories were not appreciable altered; this is consistent with TOF measurements of >4 keV ion energies. Operation with the 5:1 tube foil trap improved data collection, since end effects could be neglected. At 200 W RF power a significant decrease in deposition is observed when the foil trap is inserted as shown in Fig. 10. At higher RF power, the discharge has more sputtered neutral atoms present and becomes deposition dominated as opposed to erosion dominated due to sputtering of the helical resonator coil.

During testing we observed a variation in fast ion erosion processes for the case of pre-ionized vs. non-ionized gas breakdown (hard shot). A significant decrease in fast ion population and erosion processes at the QCM was observed with the presence of pre-ionization, suggesting a gentler, more-uniform breakdown and conduction mechanism. The ion detector located at the QCM location observed an increase in fast ion population as high as four times during the hard-shot compared to the one utilizing pre-ionization.

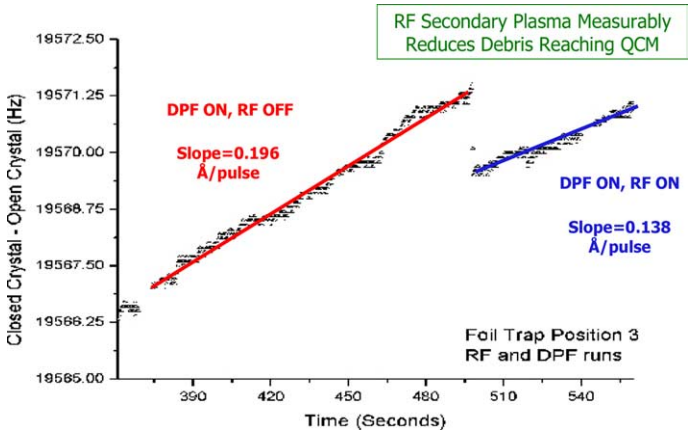

Fig. 9. Measurable reduction in debris for application of low-power 10 W RF secondary plasma with variable-aspect collimator in 3:1 position.

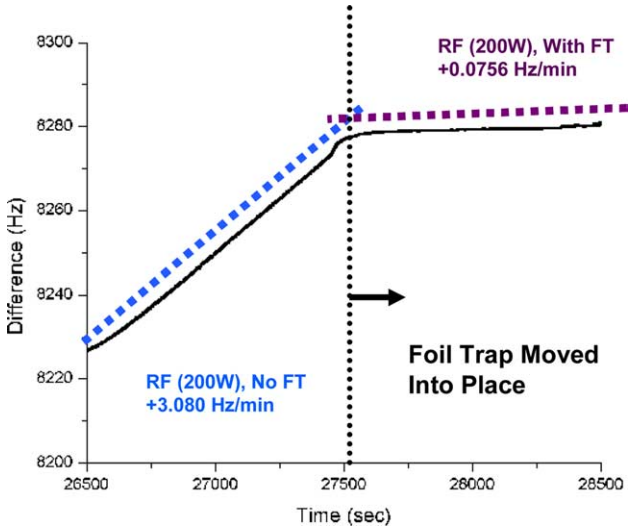

Fig. 10. Effect of grounded foil trap and RF ionization on debris indicating >97.5% debris removal rate at 200 W high power RF.

4. Summary

The operation of a dense plasma focus, secondary RF debris mitigation system, and several in situ diagnostics was achieved and debris attenuation measured. The IDEAL facility has been shown to have both an erosive fast-ion debris component and a slower deposition debris component. IDEAL will be used next to expose witness plates and optical samples to similar conditions found in commercial EUV light sources. Fast ion and fast neutral particle erosion processes at the optical mirror location will be measured and mitigation systems to slow down ions or remove these components will be developed.

Acknowledgement

This work was performed under a research grant from INTEL corp., # SRA 03–159.

References

[1] <http://www.sematech.org/resources/litho/meetings/euvl/20021014/14-Debris.pdf>, in: Proccedings of SPIE Microlithography Conference, February 2004, Santa Clara (to be published).

[2] Cymer, Inc. Available from: <http://www.sematech.org/resources/litho/meetings/euvl/20020303/04-Cymer%20020307%20ML2002Rev3.pdf>, in: Proccedings of SPIE Microlithography Conference, February 2004, Santa Clara (to be published).

[3] Xtreme Technologies. Available from: <http://www.sematech.org/resources/litho/meetings/euvl/20021014/12-Xtreme.pdf>, in: Proccedings of SPIE Microlithography Conference, February 2004, Santa Clara (to be published).

[4] Philips EUV GmbH. Available from: <http://www.sematech.org/resources/litho/meetings/euvl/20021014/09-Philips.pdf>, in: Proccedings of SPIE Microlithography Conference, February 2004, Santa Clara (to be published).

[5] D.B. Hayden, D.R. Juliano, M.N. Neumann, M.M. Allain, D.N. Ruzic, Helicon plasma source for ionized physical vapor deposition, Surf. Coat. Technol. 121 (1999) 401–404.

[6] K. Nakamura, Y. Kuwashita, H. Sugai, New inductive RF discharge using an internal antenna, Jpn. J. Appl. Phys. 34 (1995) L1686–L1688.

[7] J.P. Allain, D.N. Ruzic, Measurements and modeling of solid phase lithium sputtering, Nucl. Fusion 42 (2002) 202–210.

[8] D.N. Ruzic, Electric Probes for Low-Temperature Plasmas, AVS Monograph Series, New York, 1994.

[9] E. Vargas-Lopez, B.E. Jurczyk, D.N. Ruzic, R. Bristol, Origins of debris and mitigation through a secondary RF plasma system for discharge-produced EUV sources, Microelectron. Eng. (2004), to be published in vol. 77.